

On the dynamics of the space-charge layer inside the nozzle of a cutting torch and its relation with the “non-destructive” double-arcing phenomenon

L. Prevosto,^{1,a)} H. Kelly,^{1,2} and B. Mancinelli¹

¹Grupo de Descargas Eléctricas, Departamento Ingeniería Electromecánica, Facultad Regional Venado Tuerto (UTN), Laprida 651, (2600) Venado Tuerto (Santa Fe), Argentina

²Instituto de Física del Plasma (CONICET), Departamento de Física, Facultad de Ciencias Exactas y Naturales (UBA), Ciudad Universitaria Pab. I, (1428) Buenos Aires, Argentina

(Received 18 June 2011; accepted 8 September 2011; published online 18 October 2011)

Experimental observations on the plasma dynamics inside the nozzle of a 30 A oxygen cutting torch operated at conditions close to the double arcing are reported. It is employed a technique previously developed in our laboratory consisting in using the nozzle as a large-sized Langmuir probe. Based on the behavior of the ion current signal and simple estimations, it is concluded that (1) the non-equilibrium plasma inside the nozzle is far from the steady state in time, in contrast to what is frequently assumed. The power supply ripple was identified as the main fluctuations source and (2) large-scale plasma fluctuations inside the nozzle could cause transient (total duration of the order of 100 μ s) Townsend avalanches developing in the space-charge layer located between the arc plasma and the nozzle wall. Such events trigger the so called non-destructive double-arcing phenomena without appealing to the presence of insulating films deposited inside the nozzle orifice, as was previously proposed in the literature. © 2011 American Institute of Physics. [doi:10.1063/1.3651398]

I. INTRODUCTION

The plasma cutting process is characterized by a transferred electric arc that is established between a cathode, which is a part of the cutting torch, and a work-piece (the metal to be cut) acting as the anode.¹ In order to obtain a high-quality cut, the plasma jet must be as collimated as possible (i.e., it must have high power density). To this end, the transferred arc is constricted by a metallic tube (a nozzle) with a small inner diameter (of the order of 1 mm). A vortex-type high-pressure flow is forced through the nozzle to provide arc stability and to protect its inner wall. The intense convective cooling at the arc fringes due to the vortex flow enhances the power dissipation per unit length of the arc column, which in turn, results in high axis electric field values. Typically, arc voltage drops inside the nozzle of about 50 V or even higher are usually reached.¹

In the normal mode of torch operation, the nozzle is a floating conductor (i.e., it is not electrically connected to any part of the torch circuit). However, since the metallic nozzle itself is at a constant floating voltage, the zero current balance is fulfilled globally along the whole collecting area of the nozzle and not locally (by an ambipolar flux to the nozzle). This means that one part of the nozzle will collect electrons while the other part will collect ions. Furthermore, due to the fact that the electric current is almost carried by the electrons, the electron collecting section of the nozzle will be very little as compared to the ion collecting region. Hence, the nozzle floating potential must be close to the arc voltage at the nozzle inlet.¹ In consequence, the voltage drop between the metallic nozzle and the plasma at the nozzle exit reaches a value very close to the total arc voltage drop inside

the nozzle. Under certain operating conditions (as for instance, a too small gas mass flow), the level of arc stabilization provided by the vortex flow can be insufficient, and the arc, following the path of smallest electrical resistance (the electrical conductivity of the nozzle is much higher than that of the confined arc column), creates two separated arc channels: one from the cathode to the nozzle and another from the nozzle to the anode. Such type of arc instability is called double-arcing. From a practical point of view, the double-arcing is very undesirable, since the arc roots on the nozzle (specially the arc originated from the cathode wall) usually will destroy the nozzle almost instantaneously.

Unexpectedly, relatively little has been done to explore and understand the double-arcing phenomenon, especially considering that it is one of the main drawbacks that put limits to increasing capabilities of the plasma arc cutting process. The first hypothesis on the mechanism that triggers double-arcing in a cutting torch was formulated by Nemchinsky.² In that work, it was suggested that this mechanism consists in a Townsend avalanche developing in the cold gas layer that wraps the nozzle's orifice. This mechanism was further considered by Prevosto *et al.*^{3,4} Several obtained experimental results³ supported the Townsend avalanche hypothesis as the trigger mechanism, and suggested that it is developed in the space-charge layer that separates the plasma and the nozzle. A complementary numerical description of such space-charge layer⁴ showed that at the exit of the nozzle, the radial electric field value at the nozzle wall was higher than the radial average field across the layer. Therefore, this enhanced field could be strong enough to trigger the sheath breakdown even if the average electric field is not. In Ref. 5, Nemchinsky proposed that non-conducting films formed from eroded material from the cathode and deposited on the nozzle wall could also play a triggering role. In a recent review,⁶ high-

^{a)}Electronic mail: prevosto@waycom.com.ar.

speed images registered in cutting torches at low gas flow rates showed transient (duration < 1 ms) double-arcing events that not resulted in a nozzle destruction. This last phenomenon is still poorly understood. It was suggested in that review (in according to Nemchinsky),⁵ that such transient phenomenon (called “non-destructive” double arcing due to its short duration) was originated from a transient arc voltage spike due to insulating dielectric films deposited on the nozzle surface, which later are either carried away by the gas flow or are burned out.

Time fluctuations in thermal plasma direct-current (dc) devices are important for any technological application. A special effort has been made by several researchers (see for instance Refs. 7–9) both from an experimental or a numerical points of view to understand the dynamics of the plasma flow inside non-transferred arc torches (like spraying torches). In such torches, large plasma jet fluctuations arise either from ripple in the direct-current power supply, or random arc root movement at the anode, or combined effects of gas dynamic and electromagnetic instabilities causing cold gas entrainment. On the other hand, it is implicitly assumed in most of the experimental or numerical works in transferred arc torches (like cutting torches), that the plasma is steady.¹ However, the power sources used in such plasma torches are usually poorly stabilized and have a large ripple factor (with root-mean-square-rms-deviations that vary between $\approx 5\%$ and 10% of the mean voltage). This is due to the fact that the torch currents are of the order of 100 A, which difficult an effective filtering of the ripple. If a 3-phase transductor type of power supply is used, then the fundamental ripple frequency is 150 Hz, and if 3-phase silicon controlled rectifier based power supply is used, then the ripple frequency is 300 Hz. The strong oscillatory components in the voltage and arc current should produce in turn, large fluctuations in the plasma quantities that vary at the ripple frequency.

In this work, experimental observations on the plasma dynamics inside the nozzle of a cutting torch are reported. It is employed a technique previously developed in our laboratory consisting in using the nozzle as a large-sized Langmuir probe.³ Based on these observations and several estimations, it is presented a hypothesis according to which plasma fluctuations inside the nozzle play a key role in triggering the double-arcing phenomenon.

II. EXPERIMENTAL SET-UP

The experiment was carried out using an oxygen high-energy density cutting torch (Fig. 1). It consisted of a cathode centered above an orifice in a converging-straight copper nozzle without liquid cooling. The cathode was made of copper (7 mm in diameter) with a hafnium tip (1.5 mm in diameter) inserted at the cathode center. A flow of oxygen gas cooled the cathode and the nozzle and was also employed as the plasma gas. The gas passed through a swirl ring to provide arc stability. The nozzle consisted in a converging-straight bore (with a bore radius of 0.5 mm and a length of 4.5 mm) in a copper holder surrounding the cathode (with a separation of 0.5 mm between the holder and the cathode

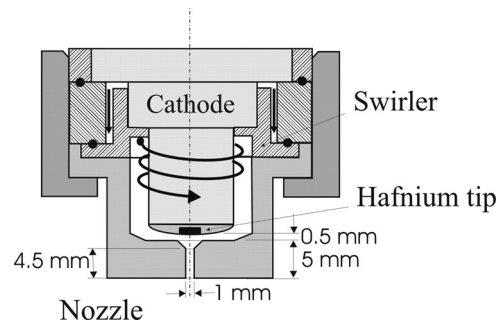


FIG. 1. Schematic of the arc torch indicating several geometric dimensions.

surface). To avoid plasma contamination by metal vapors from the anode, a rotating steel disk was used as the anode, with its upper surface located at 6 mm from the nozzle exit. A well-stabilized arc column was obtained, with the arc root sliding on the disk lateral surface. It was found that this surface resulted completely not melted (thus, practically no metal vapors from the anode were present in the arc). More details on the experimental configuration can be found elsewhere.¹⁰ A 3-phase transductor power supply with a voltage ripple level of $\approx 7\%$ and a fundamental frequency of 150 Hz was used to run the torch. The measured torch operating conditions were arc current 30 A (rms), gas mass flow rate $\dot{m} = 0.39 \text{ gs}^{-1}$, and torch chamber pressure $p_{ch} = 0.6 \text{ MPa}$. For the voltage measurements, the reference electrode was the anode (grounded) and the cathode voltage resulted in -145 V (rms).

As previously quoted, the nozzle was used as a large sized Langmuir probe. Note that the necessary condition for a comprehensive use of a Langmuir probe (i.e., the plasma should not be perturbed sufficiently far away from the probe surface) is accomplished in this case, since the nozzle-probe behaves as a natural boundary to the arc. The nozzle biasing circuit is shown in Fig. 2, and it is quite similar to the one previously employed.³ Different nozzle-anode voltage values (V_N) were obtained using a high-impedance rheostat (2 k Ω of total resistance), connected between the cathode and the

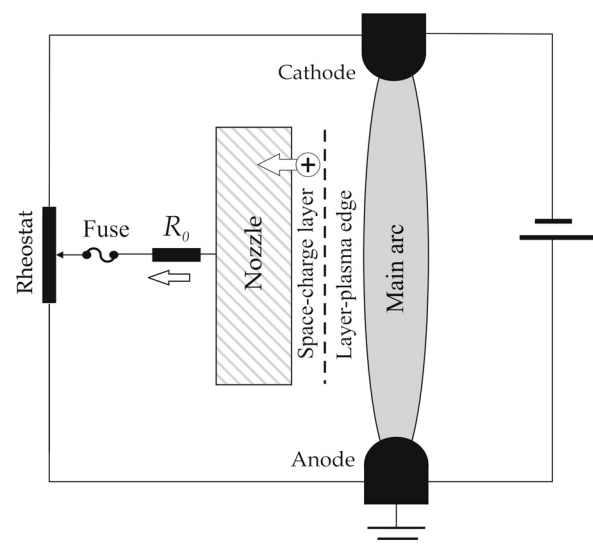


FIG. 2. Schematic of the nozzle biasing circuit.

anode of the arc, while the nozzle current (i_N) was calculated from the voltage drop through a small resistance R_0 . In practice, the nozzle was always biased so as to collect ions from the arc plasma. Since the obtained values of V_N were very close to that producing a double-arcing, a 3 A fuse was inserted in series with R_0 (see Fig. 2). In practice, a double-arcing event resulted in a blowing of the fuse instead of destroying the nozzle. Both the V_N and i_N waveforms were registered by using a two-channel digital oscilloscope (Tektronix TDS 1002 B) with a sampling rate of 500 MS/s and an analogical bandwidth of 60 MHz. For the selected value of m , double-arcing took place for a nozzle voltage close to the cathode voltage.

Finally, a set of sweeping electrostatic probes¹⁰ was used to determine the floating potential close to the nozzle exit (at 0.5 mm). The plasma potential value (V_p) at the nozzle exit was then obtained from the floating experimental value taking into account an electric field strength of ≈ 7 V/mm in the external part of the arc¹⁰ and the voltage drop between the plasma and the floating potentials (which is proportional to the plasma electron temperature). In the case we are considering, we will show later that the electron temperature is relatively low (about 5000–6000 K at the arc border) and hence such difference results of only about 5 V.

III. RESULTS AND DISCUSSION

Typical waveforms of the nozzle voltage and the ion current for an operating condition very close to double-arcing are shown in Fig. 3. It can be seen that both signals present an oscillatory component (with a main frequency of 150 Hz, which is the fundamental frequency of the power source ripple) superimposed to a mean value. The rms nozzle voltage value resulted -140 V, with a difference to the rms cathode voltage of only 5 V. For the ion signal, the rms value of the oscillatory component reaches $\approx 52\%$ of the mean value. Also, in both signals, there is a marked spike of short duration (which actually presents a complex fine structure) that was quite repetitive, appearing over many cycles of the ripple oscillation with little changes in shape. For the ion current signal, a typical spike corresponds to a peak current intensity larger than 1 A with a total time duration of the order of $100 \mu\text{s}$. A slight decrease in the nozzle voltage (to a rms value of ≈ -145 V, that is, the cathode rms value) pro-

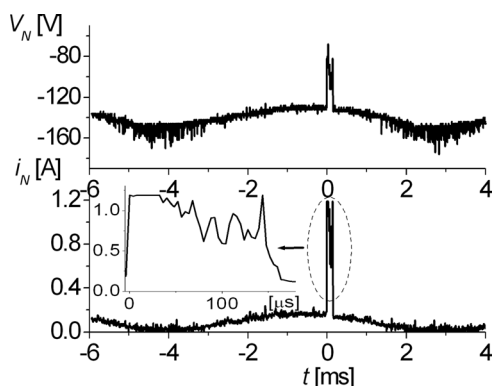


FIG. 3. Typical ion current and nozzle voltage waveforms. A speak related with the non-destructive double-arcing phenomenon is clearly recognized.

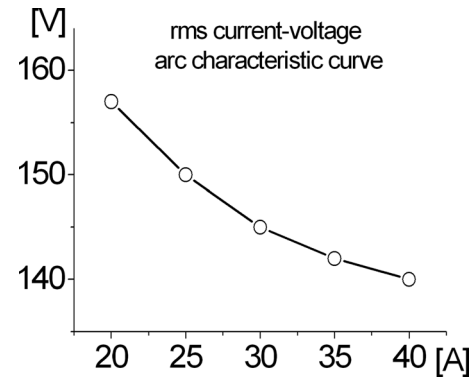


FIG. 4. RMS arc current–voltage characteristic curve of the arc torch.

duces a double-arcing with the fuse blowing. Thus, the spike suggests the presence of a non-destructive double-arcing that develops at the threshold of a double-arcing event.

In Fig. 4, it is shown the current–voltage characteristic curve of the arc torch built with RMS current and voltage values. Note that as is customary in this kind of curves, the arc voltage values were measured with respect to the cathode (instead of to the grounded anode). As expected, the characteristic curve is negative.

From the floating potential measurement close to the nozzle exit, a plasma potential mean value of ≈ -20 V (with a rms deviation of 7%) was obtained for the given arc operating conditions.¹¹

In what follows, it will be presented a physical interpretation of the ion current signal taking into account the ripple component. This interpretation is based on the use of a physical model for the space-charge layer between the arc plasma and the nozzle wall. Since the temporal variations introduced by the ripple are very slow as compared with the characteristic times in the layer (electron plasma frequency, transit time of sound perturbations along the layer, etc.), a previously developed steady model^{3,4} will be adopted, with the additional assumption that the plasma quantities follows instantaneously the arc current and arc voltage variations.

At the vicinities of the nozzle wall, the charge density will be much smaller than that at the main arc, and the electron temperature (T_e) will be well decoupled of the gas temperature T_h (close to the temperature of the nozzle wall). Following previous works,^{2–4} T_h was fixed at a value ≈ 1000 K. Although the actual T_h value is in principle very hard to obtain, the estimated value allowed obtaining a plasma-nozzle layer thickness value according to that predicted by the Paschen's breakdown law.^{3,4} Since the partial pressure due to ions and electrons is negligible compared to the gas pressure at this region,³ the time oscillations in the gas density (or pressure) can be neglected. To relate the ion current collected by the nozzle with the arc characteristics, it is necessary an evaluation of the plasma quantities at the space-charge layer-plasma boundary. The composition of this non-equilibrium plasma was calculated by using a generalized Saha-equation¹² plus the equation of state. For the first ionization,

$$\frac{n^2}{n_n} = 2 \frac{Q_i}{Q_0} \left(\frac{2\pi m k T_e}{h^2} \right)^{3/2} \exp\left(-\frac{E_I}{k T_e}\right), \quad (1)$$

$$\frac{p}{k} = T_e n + T_h (n + n_n), \quad (2)$$

(where n is the plasma density, n_n is the neutral particle density, Q_i and Q_o are the statistical weights of oxygen ions and atoms, m is the electron mass, k is the Boltzmann's constant, h is the Planck's constant, E_i is the ionization energy of the oxygen atoms, and p is the pressure). The ion current collected by the nozzle is given by

$$i_N = 2\pi R_N e \int_{z=0}^{z=L_N} \Gamma_+ dz, \quad (3)$$

(where z is the coordinate directed along the nozzle wall and R_N and L_N are the radius and length of the nozzle bore, respectively). In Eq. (3) the ion flux $\Gamma_+ = n_s v_{+s}$ must be evaluated at the edge of the plasma-layer boundary. The thickness of such a space-charge layer can be approximated in terms of the plasma-wall voltage drop ($\Delta V \equiv V_N - V_p$) as¹³

$$D \approx 2.2 \times 10^4 \Delta V^{3/5} n^{-1/2} T_e^{-1/10}, \quad (4)$$

where all the physical variables are given in MKS units. Due to the collisional regime of the layer,^{3,4} the ion entrance velocity is lower than the Bohm velocity in a factor of $(\lambda_+/\lambda_{Ds})^{1/2}$.¹⁴ (Here λ_+ is the collisional ion mean free path and λ_{Ds} is the electron Debye length at the layer entrance). Equation (4) allows to determine D at the nozzle exit, since at this position V_p is known from the floating potential measurements.

The formulation also includes the following assumptions: (i) a linear variation of the pressure (p) on z inside the nozzle; (ii) at the adjacency of the nozzle wall T_e only depends on the radial coordinate; and (iii) a constant value of the layer thickness along the nozzle. Assumptions (i) and (ii) have been shown to be valid in cutting torches.^{15,16} In any case, the obtained solution is almost insensitive to the particular chosen variations of p since the dependence of the integral in Eq. (3) with n_n is very weak (leading to a dependence of the kind $n_n^{1/8}$). Concerning the assumption (iii), it has been shown to be valid in cutting torches operated at low gas flow rates (close to double-arcing conditions).³ Note that from the assumption (iii), Eq. (4) is decoupled from Eq. (3). With all these considerations, Eqs. (1)–(3) constituted a closed system that allowed to obtain n_n , n , and T_e at the plasma-layer boundary for given values of $p(z)$ and i_N . In particular, the integral of Eq. (3) was approximated by a nine-term polynomial using the Chebyshev formula.¹⁷ Thus, the determination of n_n , n , and T_e required the solution of an inversion problem. Finally, the D value was obtained from the decoupled Eq. (4) in terms of the previously obtained plasma quantities.

In particular, Fig. 5 shows the oscillations of T_e and D corresponding to the experimental results showed in Fig. 3. Note that the T_e and D values during the spike development were not taken into account, since the assumptions employed to perform the inversion could not be valid (especially Eq. (4), which assumes that the particle creation or destruction processes can be ignored) at these times. The

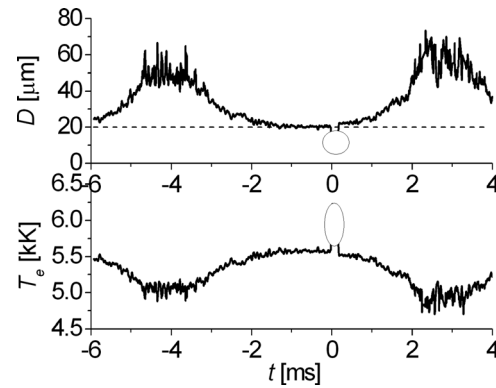


FIG. 5. The electron temperature and the thickness of the space-charge layer calculated from the experimental results showed in Fig. 3.

observed electron temperature (mean value ≈ 5400 K) shows a rms deviation $\approx 5\%$ (± 300 K), which is of the order of the arc voltage ripple level. A considerable different situation occurs with the thickness of the layer (mean value ≈ 32 μm), which presents large fluctuations. In this case, the rms deviation was $\approx 37\%$ (± 12 μm), much greater than that of T_e . This is expected because for $T_e \approx 4500$ – 6000 K, $T_h \approx 1000$ K, and $p \approx 0.1$ MPa, Eq. (1) approximately gives $n \propto T_e^\alpha$ with $\alpha \approx 15$.

The D evolution presented in Fig. 5 shows that favourable conditions for an eventual layer breakdown at times approaching to the spike exist. The dashed line in the D plot of Fig. 5 indicates the threshold D value ($\approx 19 \pm 2$ μm) for a Townsend breakdown at the nozzle exit in according to the oxygen Paschen's law¹⁷ for the given operating conditions (i.e., a mean breakdown voltage of ≈ 110 V, $T_h \approx 1000$ K, and $p \approx 1$ atm). It can be seen that the inferred D values at times approaching to the spike are very close to that threshold. Note from Fig. 3 that the spike takes place when the plasma-nozzle voltage drop is the lowest (that is, when the 150 Hz wave corresponding to V_N is close to a maximum). This behavior is related to the negative slope of the arc characteristic curve (Fig. 4) and can be explained in the following way: a small D value (close to the threshold) requires a high T_e value (see Fig. 5); but from a physical point of view, it is expected that the T_e evolution will follow the arc current evolution, while the V_N evolution will follow the arc voltage evolution. Hence, a high T_e is produced in coincidence with a high arc current value, but this high arc current is produced when the (positive) arc voltage is a minimum (negative slope of the arc characteristic) or when V_N is a maximum.

As it happens in many discharges, a Townsend breakdown along the layer will result from the development of a thermal instability.¹⁸ This eventual breakdown will likely occur at the nozzle exit, where the difference between the plasma and nozzle wall voltages ($\Delta V \equiv V_N - V_p$) is the largest. For a value of the ratio E/n_n (being E the electric field strength along the layer) below the breakdown threshold value, the particle generation inside the layer is negligible and the current in the layer being collected by the nozzle will be essentially equal to the flux of ions crossing the plasma-layer boundary. However, for increasing values of E/n_n , up to (or above) the breakdown threshold value, ionization

processes in the sheath will come into operation. For $p \approx \text{constant}$, a local increase in the gas temperature (δT_h) is accompanied with a drop in the gas density. This effect does not directly influence the field strength, but the ratio E/n_n increases. In a situation in which the unperturbed value of this ratio is close enough to the threshold one, a local increase in the gas temperature will produce a starting in the ionization processes, thus enhancing the local electrical conductivity, current density, (j) and Joule heating (jE). The gas is therefore heated even more. This thermal instability will grow if the inverse of the characteristic time for Joule heating $\nu_J = jE/(n_n c_{pl} T_h) \bar{\nu}_i$ is higher than the inverse of the characteristic time of heat removal $\nu_T = \lambda/(n_n c_{pl} \Lambda_T^2)$.¹⁸ In a general case, in which both of these competitive processes are present, the characteristic time for the growing (or quenching) of the instability will be given as $\tau \equiv |\nu_J - \nu_T|^{-1}$. (Here, $\bar{\nu}_i \equiv d \ln \nu_i / d \ln (E/n_n) = E_I \sigma_0 / (E/n_n)$ being ν_i the ionization frequency, σ_0 the cross section for elastic collisions, c_{pl} the specific heat at constant pressure per atom, λ the gas thermal conductivity, and Λ_T a length of the order of the minimal size of the volume). Since the thickness of the hydrodynamic boundary layer $\approx R_N / \sqrt{R_e}$ and D are of the same order (at the nozzle orifice, the Reynolds number (R_e) is around 500),¹⁹ ν_T involves heat conductive transport as the main heat removal mechanism inside the layer. In addition, for the layer geometry, it results $\Lambda_T \approx D$. For the unperturbed characteristic values ($T_h \approx 1000$ K, $D \approx 20 \mu\text{m}$, and $j \approx 1 \times 10^4$ A m⁻²) and for $\lambda \approx 0.1$ W (m K)⁻¹ and $\sigma_0 \approx 5 \times 10^{-20}$ m² (from Ref. 18), it follows that $\nu_J \approx 2.8 \times 10^5$ s⁻¹ $<$ $\nu_T \approx 1.1 \times 10^6$ s⁻¹ and hence $\tau \approx 1.2 \times 10^{-6}$ s. These estimations show that heat removal goes faster than Joule heating, and hence a thermal instability is quenched with a characteristic time of about 1 μm . If one assumes that the current spike is originated from a thermal instability, it is reasonable to expect that any current peak will be completely dropped in a time of the order of several τ values. The inner structure of the current spike shows several secondary peaks with durations in the range 5–15 μs (see the inset showing in detail the time evolution of the current spike in Fig. 5) so the presented estimations are in reasonable agreement with the experimental results. Another experimental evidence supporting the interpretation of the spike as the result of a quenched Townsend breakdown is the repeatability found for the spike (over many cycles of the current waveform) without ever observing a transition to a double-arcing.

IV. CONCLUSIONS

Based on the presented results, the following conclusions may be drawn:

1. The non-equilibrium plasma inside the nozzle is far from the steady state in time, in contrast to what is frequently assumed. Arc electric fluctuations due to the power source ripple exert strong influence on the characteristics of the plasma inside the nozzle of a cutting torch. In particular, the most sensitive quantity is the plasma arc-nozzle wall layer thickness that can reach values very close to those required for a Townsend breakdown along the layer.
2. By operating the cutting torch in conditions close to the formation of a double-arcing, a transient repetitive large spike (with a total duration of about 100 μs) in the ion current waveform was detected. The presence of the spike did not lead to a double arcing.
3. Large-scale fluctuations in the plasma quantities inside the nozzle could cause transient (duration of the order of 10 μs) Townsend avalanches developing in the space-charge layer. Such events will trigger the non-destructive double-arcing phenomena without appealing to the presence of insulating films deposited inside the nozzle orifice, as was proposed in the literature.

ACKNOWLEDGMENTS

This work was supported by grants from the Universidad de Buenos Aires (PID X108), CONICET (PIP 5378) and Universidad Tecnológica Nacional (PID Z 012). H.K. is member of the CONICET.

¹V. A. Nemchinsky and W. S. Severance, *J. Phys. D: Appl. Phys.* **39**, R423 (2006).

²V. A. Nemchinsky, *J. Phys. D: Appl. Phys.* **31**, 3102 (1998).

³L. Prevosto, H. Kelly, and B. Mancinelli, *J. Appl. Phys.* **105**, 013309 (2009).

⁴L. Prevosto, H. Kelly, and B. Mancinelli, *J. Appl. Phys.* **105**, 123303 (2009).

⁵V. A. Nemchinsky, *J. Phys. D: Appl. Phys.* **42**, 205209 (2009).

⁶V. Colombo, A. Concetti, E. Ghedini, S. Dallavalle, and M. Vancini, *Plasma Sources Sci. Technol.* **18**, 023001 (2009).

⁷V. Rat and J. F. Coudert, *J. Appl. Phys.* **108**, 043304 (2010).

⁸J. F. Coudert and V. Rat, *J. Phys. D: Appl. Phys.* **41**, 205208 (2008).

⁹S. Ghorui and A. K. Das, *Phys. Rev. E* **69**, 026408 (2004).

¹⁰L. Prevosto, H. Kelly, and B. Mancinelli, *IEEE Trans. Plasma Sci.* **36**, 263 (2008).

¹¹L. Prevosto, H. Kelly, and F. O. Minotti, *IEEE Trans. Plasma Sci.* **36**, 271 (2008).

¹²M. C. M. van de Sanden, P. P. J. M. Schram, A. G. Peeters, J. A. M. van der Mullen, and G. M. W. Kroesen, *Phys. Rev. A* **40**, 5273 (1989).

¹³T. E. Sheridan and J. Goree, *Phys. Fluids B* **3**, 2796 (1991).

¹⁴R. N. Franklin, *IEEE Trans. Plasma Sci.* **30**, 352 (2002).

¹⁵S. Ghorui, J. V. R. Heberlein, and E. Pfender, *J. Phys. D: Appl. Phys.* **40**, 1966 (2007).

¹⁶B. Noble, *Numerical Methods: 2 Differences, Integration and Differential Equations* (Oliver and Boyd Ltd., Edinburgh, 1964).

¹⁷R. Hackam, *J. Phys. B* **2**, 216 (1969).

¹⁸Y. P. Raizer, *Gas Discharge Physics* (Springer, Berlin, Germany, 1991).

¹⁹P. Freton, J. J. Gonzalez, A. Gleizes, F. Camy Peyret, G. Caillibotte, and M. Delzenne, *J. Phys. D: Appl. Phys.* **35**, 115 (2002).